Biochimica et Biophysica Acta 1793 (2009) 1058–1067

Contents lists available at ScienceDirect

Biochimica et Biophysica Acta

journal homepage: www.elsevier.com/locate/bbamcr

Bimodal modulation of tau protein phosphorylation and conformation by extracellular Zn^{2+} in human-tau transfected cells

Alain Boom *, Michèle Authelet, Robert Dedecker, Christelle Frédérick, Roxane Van Heurck, Valery Daubie, Karelle Leroy, Roland Pochet, Jean-Pierre Brion

Laboratory of Histology, Neuroanatomy and Neuropathology, Faculty of Medicine, Université Libre de Bruxelles, 808, route de Lennik, CP-620, B-1070 Brussels, Belgium

ARTICLE INFO

Article history:
Received 8 September 2008
Received in revised form 17 November 2008
Accepted 21 November 2008
Available online 8 December 2008

Keywords:
Alzheimer
Zinc
Tau protein
Phosphorylation
GSK-3 beta

ABSTRACT

Abnormal homeostasis of heavy metals is a well-documented physiopathological mechanism in Alzheimer's disease. An exacerbation of these abnormalities is best illustrated in the amyloid plaques in Alzheimer's disease brain tissue, in which zinc reaches the enormous concentration of 1000 μM. Zinc in the plaques is thought to originate from impaired glutamatergic neurons distributed in the associative cortex and limbic structures of normal brain. Although the characteristics of zinc binding to Aβ and its role in promotion of Aβ aggregation have been intensively studied, the contribution of zinc to the development of tau pathology remains elusive. To further document the effect of zinc we have investigated the modifications of tau phosphorylation, conformation and association to microtubules induced by zinc in clonal cell lines expressing a human tau isoform. A bimodal dose dependent effect of zinc was observed. At 100 μM zinc induced a tau dephosphorylation on the PHF-1 epitope, and at higher zinc concentrations induced the appearance of the abnormal tau conformational epitope MC1 and reduced the electrophoretic mobility of tau, known to be associated to increased tau phosphorylation. High zinc concentrations also increased glycogen synthase kinase-3β (GSK-3β) phosphorylation on tyrosine 216, a phosphorylation associated with increased activity of this tau kinase. Live imaging of tau-EGFP expressing cells demonstrated that high zinc concentrations induced a release of tau from microtubules. These results suggest that zinc plays a significant role in the development of tau pathology associated to Alzheimer's disease.

1. Introduction

Alzheimer's disease (AD) is the most common type of dementia in the elderly population. The late-onset sporadic form represents the vast majority of the cases of AD, with occurrence of rare early-onset forms of familial Alzheimer's disease caused by mutations in genes encoding for the amyloid protein precursor (APP), and presenilin 1 and 2 proteins. AD is neuropathologically characterized by the presence of neurofibrillary tangles (composed of phosphorylated tau protein) and senile plaques (containing extracellular deposits of Aβ amyloid surrounded by dystrophic neurites). Increasing evidence suggests that aberrant brain metal homeostasis is a detrimental process in AD. In particular, zinc accumulation in the neocortex has been proved to be a prominent feature of advanced AD [1] and is linked to brain amyloid Aβ peptide accumulation [2,3], enhanced formation of reactive oxygen species [4,5] and apoptosis [6]. Although physiological zinc concentration in brain interstitial space does not exceed 0.5 μM, high levels of zinc, up to 1000 μM, can be reached within amyloid plaques in AD [7]. Such pathological zinc concentrations might thus play a role in AD pathogenesis. In agreement with this hypothesis the identification of S100A6, a protein that binds zinc with a higher affinity than calcium, in a subset of astrocytes located in the amyloid plaque vicinity in both sporadic AD and in transgenic mice developing Aβ deposits, suggests that changes in expression levels of this protein might reflect some compensatory mechanisms occurring during AD progression [8,9]. Physiologically, zinc is released during glutamatergic-zinc neurons neurotransmission into the extracellular space, at the level of the synaptic cleft where the zinc concentration reaches 300 μM [10]. The zinc reuptake is achieved by non-specific neuronal presynaptic membrane transporters [11] and concentrated via a specific zinc transporter present in the synaptic glutamatergic vesicle membrane (ZnT3). In AD, the abnormal metabolism of the amyloid precursor protein (APP) leading to Aβ oligomers production and Aβ amyloid deposits could impair the normal brain metal homeostasis by interfering with the physiological zinc reuptake [12]. Moreover, zinc has been found to inhibit specifically the α-secretase cleavage of APP [13] and in concentration above 300 nM rapidly precipitates human Aβ amyloid. Zinc and Aβ amyloid acts synergistically to induce oxidative stress and extra-mitochondrial production of reactive oxygen species [14]. Thus good evidence indicates that endogenous zinc may contribute to the formation of Aβ amyloid plaques, but less is known about a potential effect of zinc on tau protein pathology although zinc has been reported to affect tau translation and phosphorylation [15] and to be present in

* Corresponding author. Tel.: +32 2 555 6505/6287; fax: +322 555 6285.
E-mail address: aboom@ulb.ac.be (A. Boom).

0167-4889/$ – see front matter © 2008 Elsevier B.V. All rights reserved.
doi:10.1016/j.bbamcr.2008.11.011

neurons containing neurofibrillary tangles [16]. The hyperphosphorylation of tau decreases the binding of tau protein to microtubules and its ability to stabilize them but also favours the formation of intracellular aggregates of tau proteins, in the form of the neuronal-paired helical filaments considered as another pathological key process in AD pathology. Tau can be phosphorylated by several protein kinases including the glycogen synthase kinase 3β (GSK-3β). GSK-3 is a multifunctional proline-directed Ser/Thr kinase [17] found ubiquitously in eukaryotes [18] and one of its isoforms, GSK-3β, is particularly abundant in the central nervous system. GSK-3β has been shown to phosphorylate tau on many sites that are hyperphosphorylated in AD, in vitro in mammalian transfected cells [19] and in transgenic animals. In this study, we have investigated the effect of zinc on tau phosphorylation and conformation and on tau binding to microtubules in cultured cells. We observed that zinc had a bimodal effect on tau phosphorylation depending on the zinc concentration, and induced GSK-3β activation and tau release from microtubules. This study shows that tau phosphorylation/conformation is modulated by zinc and suggests that the abnormally high extracellular zinc concentration present in Aβ amyloid plaques could play a role in neuronal tau pathology in AD.

2. Materials and methods

2.1. Cell culture and treatments

The 1C9 clonal CHO cells expressing stably the human 1N4R tau isoform have been previously described [20]. For life-imaging of tau distribution in cells treated or not with zinc, we generated a stable clonal CHO cell line (102C5) expressing tau conjugated to EGFP by cloning out wild-type CHO cells by limiting dilution in a selection media containing G418, after transfection with the tau-EGFP plasmid and a pSVtk neo plasmids using lipofectamine reagent (GIBCO BRL). The tau plasmid expressing the human 2N3R tau isoform conjugated to EGFP was previously described [21,22]. The cloned cell lines were analysed by Western blotting for their ability to express tau proteins and living cells examined under ultraviolet illumination to examine tau distribution. Cells were grown in HAM F12 medium supplemented with 10% foetal bovine serum, 100 IU penicillin and 100 μg/ml streptomycin and incubated at 37 °C with a 95% air/5% CO_2 mixture. Cultured cells were treated for 4 h with zinc by adding to the culture medium zinc sulphate (Sigma, USA) from a stock solution (100 mM) to obtain a final range of concentrations of 100, 150, 250 and 500 μM. Cultured cells were also treated with 10 μM of the specific glycogen synthase kinase-3 inhibitor SB-216763 (Torcis, United Kingdom), in absence or in presence of zinc.

2.2. Cell viability: 3-(4,5-dimethyl-thiazoyl-2-yl)2,5diphenyltetrazolium bromide (MTT) assay

1C9 cells were cultured in 96-well plates, and after reaching confluency treated for 4 h with 100–500 μM zinc sulphate. Twenty five microliters of MTT solution (5 mg/ml) was then added to the media, and the cells further incubated for 4 h at 37 °C. The MTT formazan product was solubilized with an appropriate solution. Optical densities were measured at 570 nm.

2.3. Antibodies

The rabbit polyclonal anti-tau antibody B19 was raised against bovine tau proteins and reacted with human and rodent tau proteins [23]. This antibody recognizes different tau isoforms both phosphorylated and unphosphorylated. The mouse monoclonal antibody PHF1 recognizes a specific epitope on the tau protein in a phosphorylation-dependent manner, i.e. its reactivity with tau proteins is dependent of the phosphorylation of Ser396/404 [24]. The monoclonal MC1 antibody recognizes an abnormal tau conformational epitope [25]. The mouse monoclonal antibody TPK1 (Becton Dinkinson, USA) is specific for GSK-3β and the rabbit polyclonal anti-GSK α/β (Biosource, Belgium) is specific for active forms of GSK-3α phosphorylated on tyrosine 279 and for GSK-3β phosphorylated on tyrosine 216. The mouse monoclonal antibodies to α-tubulin (clone DM1-A), and to β-actin (clone AC15) were purchased from Sigma (Bornem, Belgium).

2.4. Whole cell homogenate preparations

Cultured cells treated or not treated for 4 h with 100–500 μM zinc sulphate were homogenized on ice in a buffer (Tris 50 mM, EDTA 10 mM, NaCl 100 mM, pH 7.4) containing protease and phosphatase inhibitors (1 mM phenylmethylsulphonyl-fluoride (PMSF), leupeptin 25 μg/ml, pepstatin 25 μg/ml, Na_3VO_4 1 mM, NaF 20 mM). The amount of proteins in homogenates was estimated with the Bradford method (Bio-Rad reagent, USA).

2.5. Western blotting

Homogenates of cultured 1C9 cells, treated or not for 4 h with 100–500 μM of zinc sulphate were analysed by sodium dodecyl sulphate-polyacrylamide (10%) gel electrophoresis (SDS-PAGE). The extracts were first mixed with a sample buffer (10 mM Tris–HCl, pH 6.8, 1.5% SDS, 0.6% DTT and 6% (v/v) glycerol) and heated at 95 °C for 2 min. After separation, proteins were electrophoretically transferred to nitrocellulose membranes. Nitrocellulose membranes were blocked in non-fat milk (10% (w/v) in TBS) for 1 h at room temperature and incubated with the primary antibody overnight, followed by either anti-mouse or anti-rabbit immunoglobulins conjugated to biotin, followed by streptavidin conjugated to alkaline phosphatase. Membranes were finally incubated in the developing buffer (Tris 0.1 M, NaCl 0.1 M, $MgCl_2$ 0.05 M, pH 9.5) containing nitro blue tetrazolium and 5-bromo-4-chloro-3-indolyl phosphate. The densitometry analysis of western blots was performed with the Image J 1.34 program (NIH, USA).

2.6. Immunocytochemistry

Cultured 1C9 cells treated or not for 4 h with 100–500 μM zinc sulphate were rinsed in TBS (0.01 M Tris, 0.15 M NaCl, pH 7.4) buffer and fixed for 10 min in 4% (w/v) paraformaldehyde in 0.1 M phosphate buffer, pH 7.6. Tau immunohistochemical labelling was performed using the avidin–biotin-peroxidase complex (ABC) method. Briefly, fixed cells were incubated for 1 h at room temperature with the blocking solution diluted in TBS (5% (v/v) of goat or sheep normal serum (depending on the origin of the secondary antibody). After an overnight incubation with the anti-tau antibodies (B19 1/3000; PHF1 1/50.000, the 1C9 cells were sequentially incubated with the appropriate secondary antibodies reagents (Vector Laboratories, The Netherlands) conjugated to biotin (1:100) followed by the avidin–biotin peroxidase complex (Vector Laboratories, The Netherlands). The peroxidase activity was revealed using diaminobenzidine as chromogen. Immunofluorescence using anti-tau antibodies was also performed on 1C9 cells grown on coverslips. The coverslips were rinsed with Tris-buffered saline (TBS) and fixed with 4% of paraformaldehyde in TBS, permeabilized with 0.15% Triton X-100 in PBS for 10 min and washed three times with TBS. The fixed cells were preincubated for 1 h at room temperature with 1:30 normal serum in TBS. Incubation with the anti-tau antibodies (B19 and PHF1 and MC1) was performed overnight. After washing in TBS, the cells were incubated 1 h in the dark with the fluorescein-labelled secondary antibody at 1:30 dilution. Cells were again washed three times in PBS for 10 min, rapidly rinsed with distilled water, and mounted with Mowiol mounting medium (Calbiochem, USA) solution containing 100 mg/ml DABCO reagent (Sigma, USA). Cells were observed under a Zeiss Axiovert fluorescence microscope equipped with a Laser-Scanning Confocal Microscope (MRC 1000, BioRad) using an argon–krypton laser.

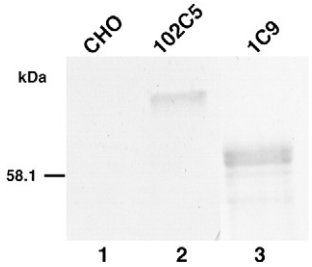

Fig. 1. Characterisation of tau expression in CHO cell lines used in this study. Homogenates of wild-type CHO cells (lane 1), clonal 102C5 cells (lane 2) and clonal 1C9 cells (lane 3) were analysed by western blotting with the B19 pan-tau antibody. Wild-type CHO cells do not express tau proteins. 1C9 cells express a 1N4R tau isoform and 102C5 cells a higher molecular weight 2N3R tau isoform conjugated to EGFP. The number on the left refers to the position of a molecular weight marker (58 kDa: catalase).

2.7. $[Zn^{2+}]_i$ measurement

For measurement of intracellular zinc, 1C9 cells were first washed twice with Hepes buffer (10 mM Hepes, 150 mM NaCl, 5 mM KCl, 1 mM $MgCl_2$, 5 mM glucose, 4 mM glutamine, and 1.8 mM $CaCl_2$, pH = 7.4) and then loaded with 2 μM FuraZin acetoxymethyl ester (a fluorescent probe for zinc) (Molecular Probes, USA) in Hepes buffer for 30 min at 37°C. After loading with this fluorescent probe, the cells were incubated in Hepes buffer for 15 min to allow complete de-esterification of the dye. Coverslips with loaded cells were mounted in a 1 ml thermostated (37 °C) open chamber placed on an Olympus inverted microscope as previously described [26]. Zinc sulphate was added to the chamber in a volume of 100 μl Hepes buffer. Changes in FuraZin fluorescence in individual cells were measured by ratio fluorometry using a camera-based TillVision imaging system (Till Photonics, Gräfelfing, Germany). Fluorescence signals emitted at 550 nm after excitation at 340 and 380 nm were measured, and ratio values were calculated.

2.8. Live-imaging observation of tau-EGFP expressing cells

The effect of treatment with 250 μM zinc sulphate on the microtubule network of cultured cells was analysed by time-lapse imaging of 102C5 cells (expressing an 2N3R human tau-EGFP isoform). Cultured 102C5 cells were incubated at 37 °C with a 5% CO_2/95% air mixture in a thermostatic chamber placed on the stage of

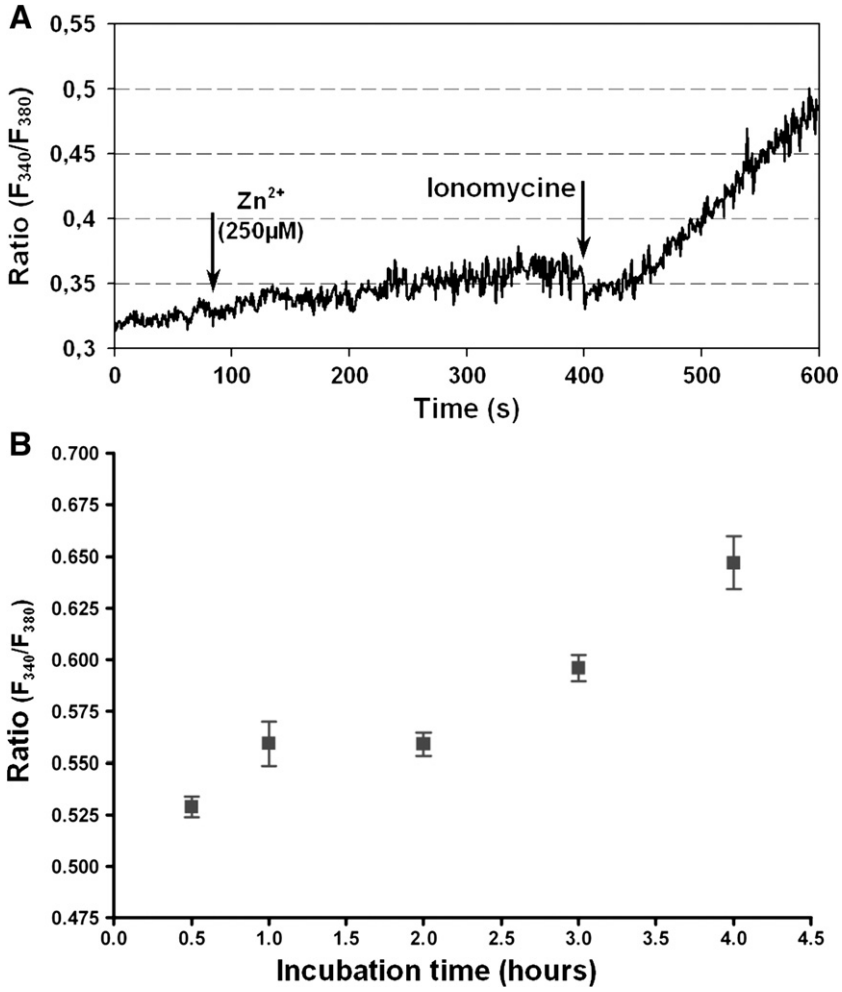

Fig. 2. Measurement of zinc accumulation by spectrofluorometry experiments performed on 1C9 cultured cells. (A) Cells were loaded with FuraZin and incubated during 300 s in presence of 250 μM zinc sulphate (first arrow on the time axis) and a ratio measurement (R = F340 nm/F380 nm) was performed every second and plotted in a time vs. ratio graph. The ratio curve increased linearly as a function of the incubation time to reach 120% of initial value, indicating moderate entry of zinc during this incubation period. At the end of the 300 s incubation period, ionomycine was added to the culture medium and ratio values (F340 nm/F380 nm) were measured for another 200 s and plotted in the same graph. Ionomycine induced an important increase in zinc entry, characterized on the graph by a slope increase. (B) The increase in Zn^{2+} absorption by 1C9 cells was determined by measuring fluorescence emission of FuraZin loaded cells. Measurements were performed at 0.5, 1, 2, 3 and 4 h after adding 250 μM zinc sulphate (final concentration). Since no Zn^{2+} is present in resting cell, no recording was performed at time 0 h. Data are given as ratio of emitted light at 340 nm and 380 nm excitation. Values are averaged from at least 11 cells from 2 independent experiments (mean ± SEM). Zinc accumulated steadily in cells during the 4 h incubation period.

an inverted Zeiss Axiovert 200 M microscope equipped with an Axiocam MR black and white camera. Digital images were automatically captured every 10 min during a 4 hour period using the Axiovision software (Zeiss, Germany).

3. Results

3.1. Tau expression in cell lines

Tau expression in the cell lines used in this study was analysed by western blotting. As reported previously, wild-type CHO cells do not express tau proteins whereas clonal 1C9 cells expressing a single tau isoform show a major species with an apparent molecular weight of 60 kDa (Fig. 1, lane 3) [20]. The clonal 102C5 cells express a tau isoform conjugated with EGFP and with an apparent higher molecular weight (Fig. 1, lane 2). Life 102C5 cells examined under ultraviolet illumination showed a fluorescent microtubule network, due to the binding of tau-EGFP to microtubules (Fig. 8).

3.2. Cell viability

As estimated by the MTT tests, zinc sulphate treatment did not induce any significant toxicity in human tau CHO transfected cells using up to 500 μM concentration during a four-hour-time incubation (data not shown).

3.3. Spectrofluorometry confirms zinc entry into cultured cells

Spectrofluorometry experiments were carried out to ensure that zinc penetrates and accumulates into the cultured cells. To this end, two experiments were performed on 1C9 cells. In the first one cells loaded with FuraZin were incubated with 250 μM zinc sulphate. The 340 nm/380 nm ratio increased linearly as a function of the incubation time to reach 120% of the initial value after 300 s of incubation (Fig. 2A), indicating a moderate entry of zinc into cells even during this short period. To confirm that the increase in ratio values was due to zinc entry, ionomycine was added at the end of the incubation period of 300 s. Measurements of ratio values showed an important increase in zinc entry, characterized on the graph by a steeper slope (Fig. 2A). In a second experiment, cells were incubated for 0 h, 0.5 h, 1 h, 2 h, 3 h and 4 h in a medium containing 250 μM zinc. Cells were then washed and loaded with 2 μM Furazin. Five snapshots were taken at both excitation wavelengths (340 nm and 380 nm) and averaged ratios values calculated. The ratio value started at 0.525 and reached a value of 0.650 after 4 h (Fig. 2B), confirming zinc steadily accumulation into cells on longer period, comparable to zinc entry observed on a shorter period with an ionophore.

3.4. Zinc induces modifications of tau expression and phosphorylation

In order to determine the effect of zinc on tau expression and phosphorylation, 1C9 cells were treated during 4 h with increasing

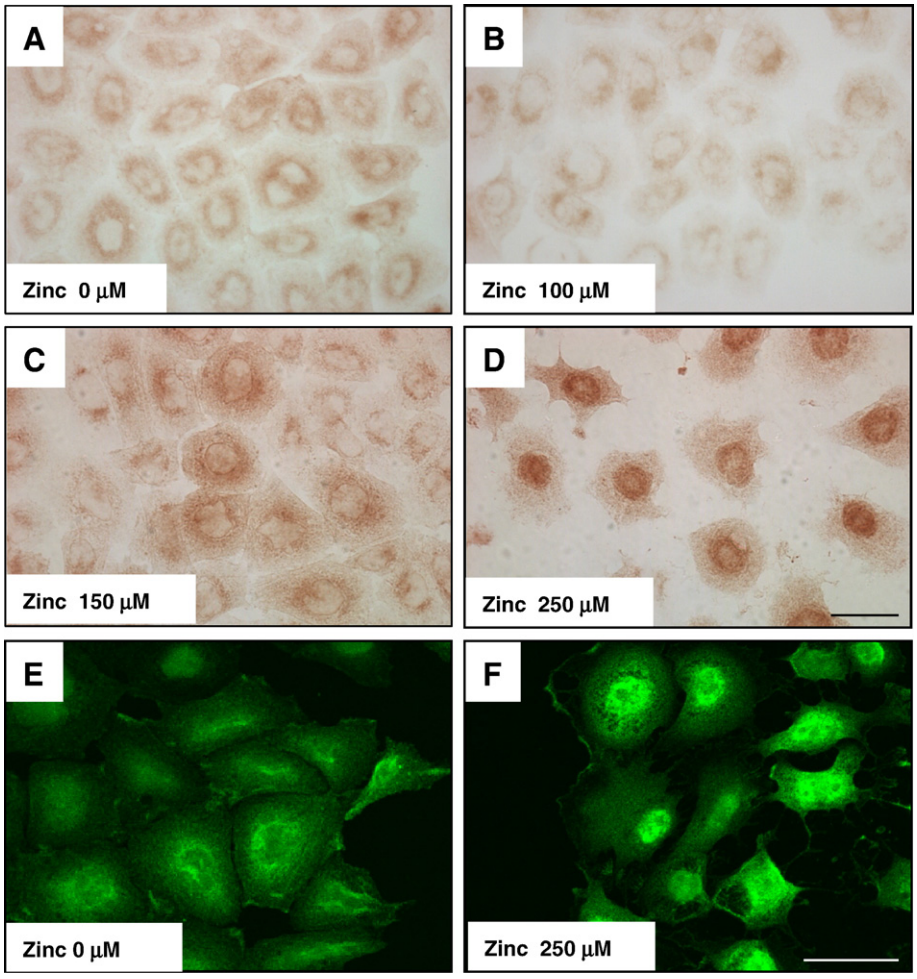

Fig. 3. Photomicrographs of immunocytochemical labelling (no counterstaining) with the phosphotau antibody PHF-1 on control 1C9 cells (A and E) and 1C9 cells treated with zinc sulphate for 4 h (B–D and F). (A and B) Control 1C9 cells showed a moderate cytoplasmic PHF-1 labelling, whereas 1C9 cells treated for 4 h with 100 μM zinc sulphate showed a decrease in PHF-1 immunoreactivity (B). (C and D) On the contrary, increased PHF-1 labelling was observed when the cells were incubated with 150 μM (C) and 250 μM of zinc sulphate (D). Under this latter condition a nuclear labelling for tau was also observed. (E and F) Immunofluorescence pictures of the PHF-1 labelling obtained with a confocal microscope. Untreated 1C9 cells (E) showed a reticular staining throughout the cell whereas cells treated with 250 μM of zinc sulphate (F) showed an increased labelling. Scale bar: 25 μM.

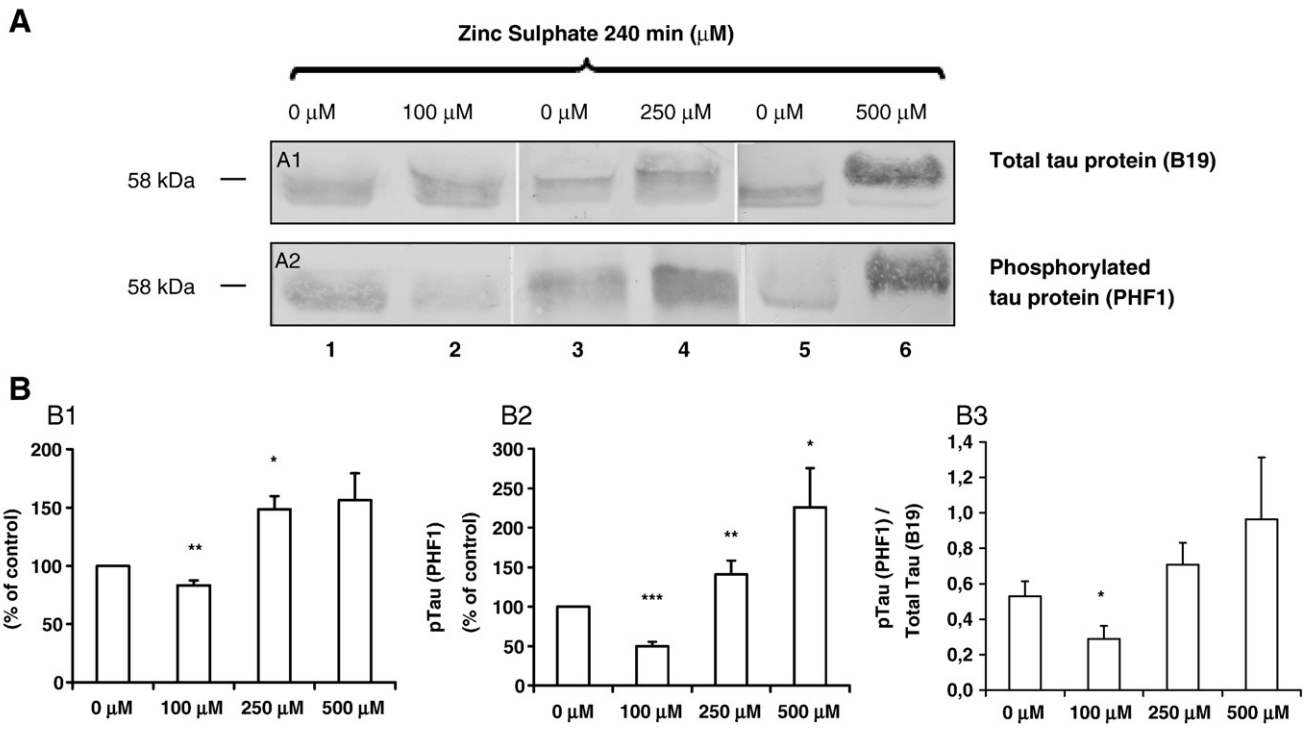

Fig. 4. Effect of zinc sulphate on tau expression and PHF-1 phosphotau immunoreactivity. (A) Immunoblotting of total cell lysates (100 μg/lane) from 1C9 cells treated or not with different zinc sulphate concentration and probed with the B19 antibody recognizing both phosphorylated and unphosphorylated tau (panel A1) or with the phosphorylation-dependent monoclonal tau antibody PHF-1 (panel A2). 1C9 cells exposed to 250 and 500 μM zinc sulphate showed an apparent increase of tau expression and a reduced electrophoretic mobility when probed with the B19 tau antibody (panel A1). 1C9 cells exposed to 100 μM zinc sulphate and probed with the PHF-1 tau antibody showed a decrease in tau phosphorylation (panel A2—100 μM). In contrast, incubation with higher zinc sulphate concentrations led to an apparent increase in PHF-1 tau immunoreactivity. The number on the left refers to the position of a molecular weight marker (58 kDa: catalase). (B) Densitometry quantifications performed on eight independent experiments. Decreased tau expression and PHF-1 phosphotau was statistically significant for 100 μM zinc (panel B1) and increased tau expression and PHF-1 phosphotau was significant for 250 μM (panel B2) (as means ± SEM, relative to controls). Calculated PHF-1/total tau (B19) ratios were statistically significant for 100 μM zinc sulphate (panel B3). $*p<0.05$; $**p<0.01$. ANOVA with post tests for comparison with control cells.

zinc concentrations and analysed by immunocytochemistry and immunobloting with tau antibodies. In the absence of zinc sulphate, a weak cytoplasmic immunostaining by the phosphorylation-dependent anti-tau antibody PHF1 could be observed (Fig. 3A — Control). PHF1 immunolabelling was clearly decreased when the cells were incubated 4 h with 100 μM zinc sulphate (Fig. 3B—100 μM). In

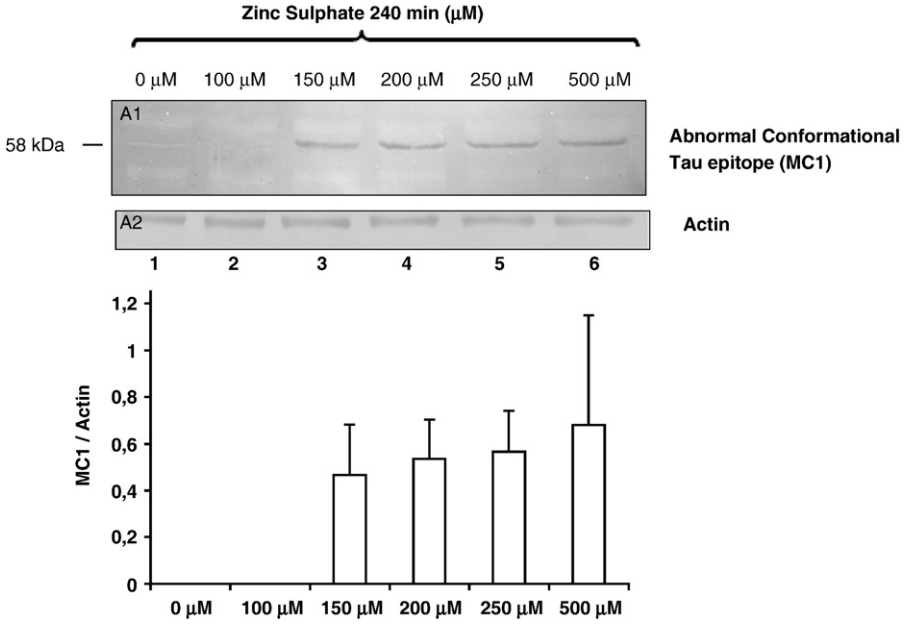

Fig. 5. Effect of zinc sulphate on the appearance of the abnormal MC1 tau conformational epitope. (A) Immunoblotting of total cell lysates (100 μg/lane) from 1C9 cells with the conformational MC1 tau antibody (panel A1) or an anti-actin antibody (panel A2). A MC1 immunoreactivity was absent when 1C9 cells were incubated in the absence or with low (100 μM) zinc sulphate concentration. In contrast, at 150 μM or higher zinc sulphate concentrations, a MC1-positive tau species was observed. The number on the left of the panel indicates the position of the molecular weight marker (58 kDa: catalase). (B) Densitometry quantification of the MC1/actin ratios, that increased sharply for zinc sulphate concentrations above 100 μM.

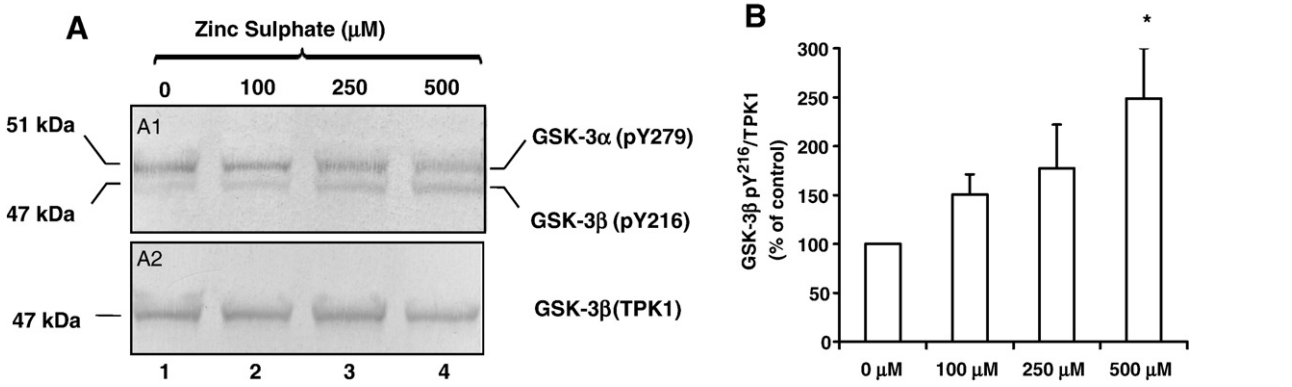

Fig. 6. Effect of zinc sulphate on GSK-3β phosphorylation. (A) Immunoblotting of 1C9 cell lysates with the anti-GSK 3β/α [pY216] antibody (panel A1) or the total anti-GSK-3β antibody TPK1 (panel A2). Treatment with 250 and 500 μM of zinc sulphate increased the level of GSK-3β phosphorylated on tyrosine 216 [pY216] whereas the phosphorylation of GSK-3α [pY279] and the level of total GSK-3β (TPK1) were not affected. (B) Densitometry quantification of GSK-3β [pY216]/total GSK-3β ratios following treatment with different zinc concentration from three independents experiments (expressed as mean ± SEM, relative to controls). Numbers on the left of panels A1 and A2 indicate the position of GSK-3α (51 kDa) and GSK-3β (47 kDa). *$p<0.05$, compared with controls by one sample t test.

contrast, cells exposed to higher zinc sulphate concentrations showed an increase in PHF1 immunolabelling (Fig. 3C and D). A nuclear PHF-1 immunolabelling of fixed 1C9 cells was also observed after incubation with 250 μM zinc (Fig. 3D). Immunofluorescence observation with confocal microscopy confirmed the increased PHF-1 labelling in 1C9 cells in the presence of 250 μM zinc sulphate (Fig. 3E and F). These modifications in PHF-1 immunolabelling of 1C9 cells exposed to zinc sulphate were confirmed by immunoblotting experiments. Homogenates of 1C9 cells exposed to 100 μM zinc sulphate showed a decrease in PHF-1 tau immunoreactivity (Fig. 4A, panel A2, lane 2). Incubation with higher zinc sulphate concentrations led to an increase in PHF-1 immunoreactivity (Fig. 4A, panel A2, lanes 4 and 6). Incubation with 250 μM and 500 μM zinc sulphate also decreased the electrophoretic mobility of tau (Fig. 4A, panel A1, lanes 4 and 6), a reported electrophoretic behaviour associated to selected changes in tau phosphorylation [27,28]. The total level of tau estimated with the

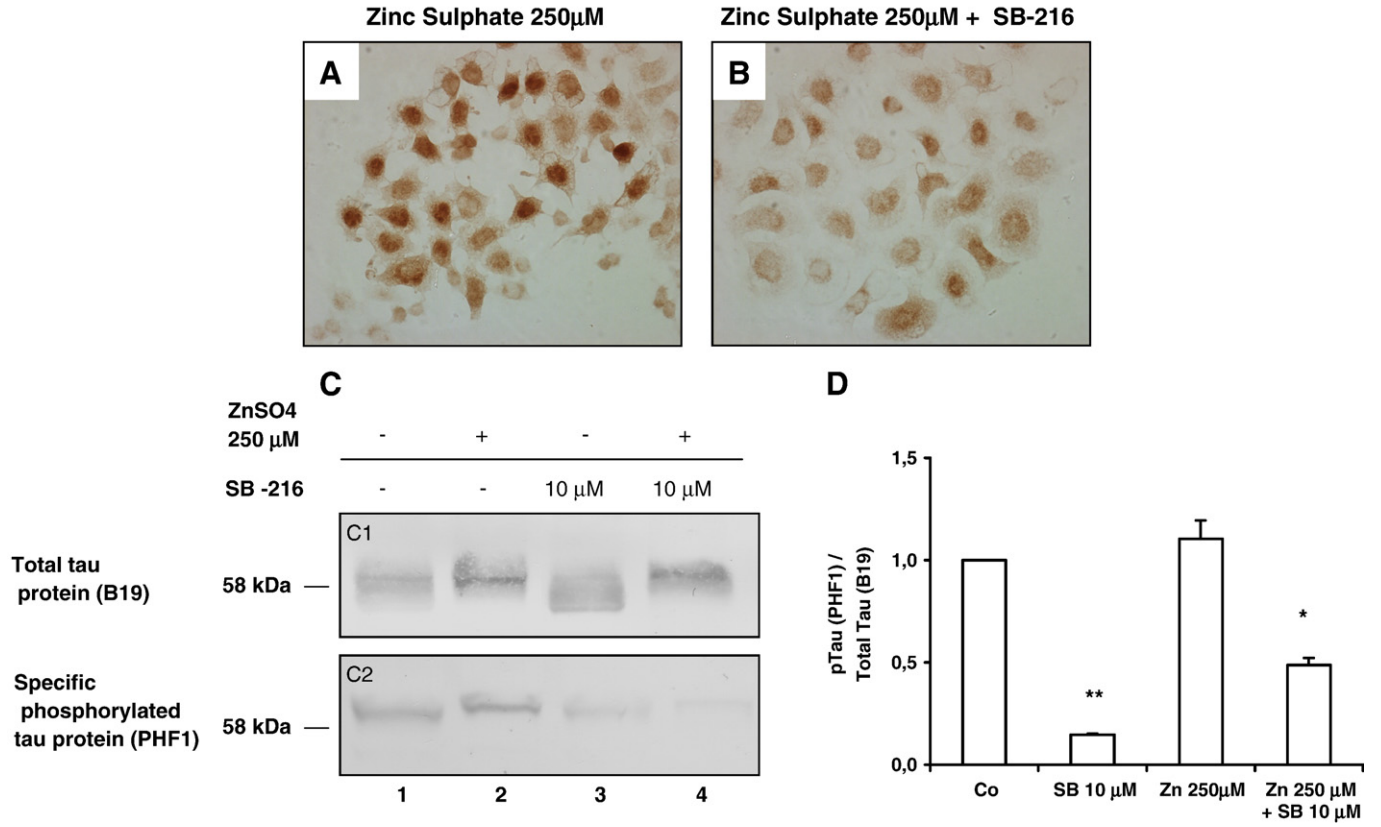

Fig. 7. Effect of the GSK-3β inhibitor SB-216763 on PHF-1 tau immunoreactivity and tau electrophoretic mobility in presence of 250 μM zinc sulphate. (A and B) A strong PHF-1 labelling is observed in 1C9 cells incubated with 250 μM zinc sulphate (A) and addition of 10 μM of SB-216763 led to a reduction of PHF-1 immunoreactivity in zinc-treated cells (B). (C) Immunoblotting of 1C9 cell lysates with the B19 total tau antibody (panel C1) and the PHF-1 tau antibody (panel C2). A reduction in electrophoretic mobility of tau and of PHF-1 immunoreactivity is present in cells treated with zinc (lanes 2) or with zinc and SB-216763 (lanes 4). (D) Densitometry quantification of PHF-1/B19 ratios from three independents experiments. A significant decrease is present in cells treated with SB-216763 or to a lesser extent with zinc and SB-216763. *$p<0.05$; **$p<0.01$. ANOVA with post tests for comparison with control cells.

phosphorylation independent B19 antibody was however also observed to be increased in 1C9 cells treated with 250 and 500 μM zinc sulphate (Fig. 4A, panel A1). The densitometry quantification of total tau (B19) (Fig. 4B, panel B1) and of PHF-1 phosphotau (Fig. 4B, panel B2) confirmed the decrease of PHF-1 immunoreactivity at 100 μM zinc sulphate and the increase of tau expression and of PHF-1 immunoreactivity after incubation with 250 and 500 μM zinc sulphate. The calculated PHF1/B19 densitometry ratios (Fig. 4B, panel B3) indicated a significant decrease of this ratio for 100 μM zinc sulphate but these ratios were not significantly different for higher zinc sulphate concentrations, despite a trend for increased values.

3.5. Zinc induces the appearance of the MC1 tau conformational epitope

By immunoblotting we then examined the effect of zinc sulphate on the appearance of modified conformational epitopes on tau, using the conformational MC1 tau antibody that recognizes a discontinuous epitope on the tau molecule and considered as one of the earliest pathological alterations of tau in AD. MC1 immunolabelling was undetectable in untreated 1C9 cells or in cells treated with 100 μM zinc sulphate (Fig. 5A, panel A1, lanes 1 and 2), but an obvious MC1 positive tau species was detected at 150 μM or at higher zinc sulphate concentrations (Fig. 5, panel A1, lanes 3 to 6).

3.6. Zinc induces GSK-3β phosphorylation on tyrosine 216

Immunoblots of total cell lysates from 1C9 cells exposed to different extracellular zinc sulphate concentrations and probed with the anti-GSK 3β/α [pY216] antibody showed an increased level of GSK-3β phosphorylated on tyrosine 216 [pY216] for the highest zinc concentration (250 and 500 μM) (Fig. 6A, panel A1, lanes 3 and 4). Phosphorylation of GSK-3α [pY279] (Fig. 6A, panel A1) and expression of total GSK-3β (estimated with the TPK1 antibody) (Fig. 6A, panel A2) were not affected by zinc treatments. The calculated GSK-3β [pY216]/total GSK-3β densitometry ratios are shown in Fig. 6B and indicate a significant increase for the highest zinc sulphate concentration.

The effect of SB-216763, a specific inhibitor of GSK-3β, was investigated to determine if GSK-3β was involved in modifications in phosphorylation and electrophoretic mobility of tau in cells treated by higher zinc sulphate concentrations. Treatment with SB-216673 decreased PHF-1 immunoreactivity of cells treated with zinc (Fig. 7A versus B). By immunoblotting tau phosphorylation detected by the PHF1 antibody in the absence of zinc was strongly reduced by treatment with SB-216763 (Fig. 7C, panel C2, lane 1 vs. lane 3). In presence of zinc, PHF-1 tau immunoreactivity was also reduced by treatment with SB-216763 (Fig. 7C, panel C2, lane 2 vs. lane 4) and reduced tau electrophoretic mobility induced by zinc was almost not affected by SB-216763 (Fig. 7C, panel C1, lane 2 vs. lane 4). The calculated PHF-1/total tau (B19) densitometry ratios of three independent experiments are shown in Fig. 7D and indicate a significant decrease of PHF-1 tau immunoreactivity in cells treated with SB-216763, both in absence or presence of zinc. These results thus suggest that GSK-3β maintains tau PHF-1 immunoreactivity in cells treated with zinc but is not responsible for the reduced electrophoretic mobility of tau in these cells.

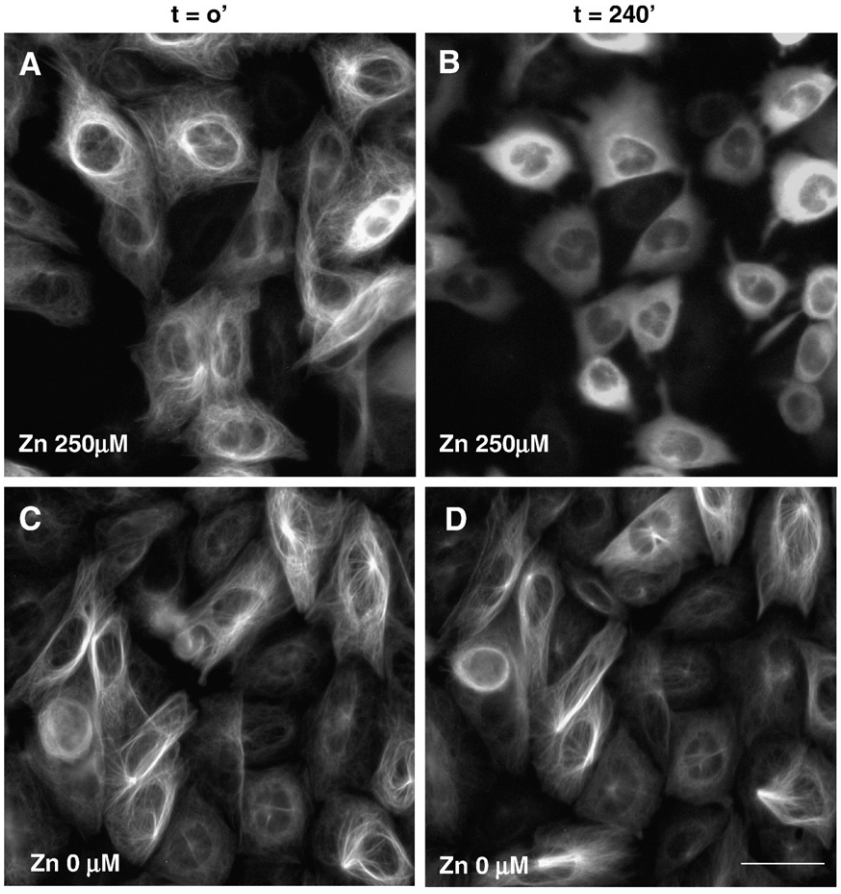

Fig. 8. Effect of zinc on tau association to microtubules studied by time-lapse imaging in life clonal 102C5 cells. (A and B) Cells treated with 250 μM zinc sulphate. At the start of the time-lapse observation ($t = 0'$) (A), cells expressing tau conjugated to EGFP show a fluorescent microtubule network, due to the association of the tau-EGFP proteins to microtubules. Zinc treatment led to a progressive disappearance of the microtubule network that was replaced after 4 h ($t = 240'$, last record of the time-lapse observation) by an uniform tau fluorescence throughout the cell cytoplasm (B). (C and D) Control untreated cells. Time-lapse imaging showed the persistence of the microtubule network from the start (C) to the end (D) of the time-lapse observation. Scale bar: 15 μM.

3.7. Time-lapse imaging shows a release of tau from microtubules in zinc-treated cells

To further document the change in cellular distribution of tau induced by zinc, the effect of 250 μM zinc sulphate was analysed by time-lapse imaging on living CHO cells expressing a human tau-EGFP isoform (Clone 102C5). Before zinc sulphate addition, cells showed a fluorescent fibrillar pattern corresponding to the microtubule network, due to the association of the tau-EGFP proteins to microtubules (Fig. 8A). The addition of 250 μM zinc led progressively in 4 h to the disappearance of the fluorescent microtubule network that was replaced by an uniform tau fluorescence throughout the cell (Fig. 8B). 102C5 cells untreated with zinc were examined in parallel by time-lapse imaging. These untreated cells did not show a disappearance of the fluorescence microtubular network after a period of 4 h of time-lapse imaging (Fig. 8C and D). This fluorescence pattern suggested that tau-EGFP proteins were detached from microtubules and/or that microtubules were depolymerised in presence of zinc.

3.8. The microtubule network is still present in zinc-treated cells

To further document the integrity of the microtubule network in zinc-treated cells, 102C5 cells were immunolabelled with the anti-α-tubulin antibody after treatment with zinc sulphate. The microtubule network present in untreated cells (Fig. 9A) was still present in cells treated for 4 h with 150 (Fig. 9B) or 250 μM (Fig. 9C) zinc sulphate.

4. Discussion

Elevated intracellular free zinc (i.e. zinc ions not complexed to intracellular proteins) is neurotoxic and its accumulation may contribute to neuronal injury in several diseases, including in neurodegenerative conditions such as Alzheimer's disease. Aberrant zinc metal homeostasis has been reported in the brains of AD patients and this metal could contribute to the development of the lesions [1]. Although much evidence indicates that zinc enhances the development of amyloid pathology in AD [12,29,30], the effect of zinc on the development of tau pathology has been studied only in few studies [15]. The present study shows that tau phosphorylation and conformation is modulated by zinc in a concentration dependent manner in a cellular model. The intracellular concentration of free zinc is normally low and elevation of intracellular zinc results from entry through calcium permeable channels [31]. Our spectrofluometric analysis confirmed that zinc ions added extracellularly entered and accumulated into cultured cells in our experimental conditions.

Interestingly, we observed a bimodal evolution of tau phosphorylation and an abnormal epitope conformation when using increasing concentration of zinc sulphate. At the lowest zinc concentration of 100 μM, tau phosphorylation at Ser396/404, identified by the PHF-1 antibody, decreased significantly. Tau dephosphorylation induced by zinc could result from either activation of protein phosphatases or inhibition of protein kinases e.g. zinc has been reported to inhibit GSK-3β in vitro in an uncompetitive manner, with an almost complete inhibition at 100 μM [32], suggesting that tau dephosphorylation observed in these cells might be mediated by direct GSK-3β inhibition. For zinc concentration higher than 100 μM we observed an increase of PHF-1 immunoreactivity but that probably reflected a parallel increase in tau expression. This effect was also observed in a previous study [33], and attributed to an increased activity of a 70 kDa ribosomal protein S6 kinase regulating protein translation. We also observed that high concentrations of zinc actually increased phosphorylation of GSK-3β on Tyr216, a phosphorylation event associated to increased activity of GSK-3β [34]. GSK-3β has been observed to be associated to neuronal lesion in AD [34] and the level of GSK-3β phosphorylated on Tyr 216 (an active form of the enzyme) increases in AD [35]. In addition, for zinc concentration above 100 μM, we detected a conformational change in tau by using the conformational MC1 antibody, which recognizes a discontinuous epitope along the tau molecule [25]. Interestingly, the appearance of the MCI epitope is considered as one of the earliest pathological alterations of tau in AD [25]. Another indication of increased tau phosphorylation and conformational change for zinc concentrations above 100 μM was its reduced electrophoretic mobility, a reported electrophoretic behaviour associated to increased tau phosphorylation [27]. This increased tau phosphorylation could be directed at other sites than the PHF-1 site (Ser 396/404), e.g. phosphorylation at Ser202/Thr205, known to reduce electrophoretic mobility of tau [28]. This reduced electrophoretic mobility induced by zinc was not affected by co-treatment with a GSK-3β inhibitor, suggesting that GSK-3β was not primarily involved in the zinc-induced reduced electrophoretic mobility of tau. The presence of a nuclear tau immunoreactivity in fixed cells, although reminiscent of previous observations reporting the presence of neuronal nuclear tau in AD brains [36], should be interpreted with caution since it was not observed by life imaging of cells expressing tau-EGFP, and we cannot exclude that it represents a redistribution of tau during fixation [37]. By time-lapse imaging using cells expressing tau-EGFP we observed that 250 μM of zinc causes also an intracellular redistribution of tau protein with the disappearance of its association to the microtubule network, the latter being still present in these zinc-treated cells. Binding of tau to microtubules is regulated through phosphorylation and increased GSK-3β activity reduces the association of tau with microtubules [38,39]. In a previous study [33], an increase of tau phosphorylation was reported when SH-SY5Y cells were treated with a single concentration of 100 μM of zinc in serum-

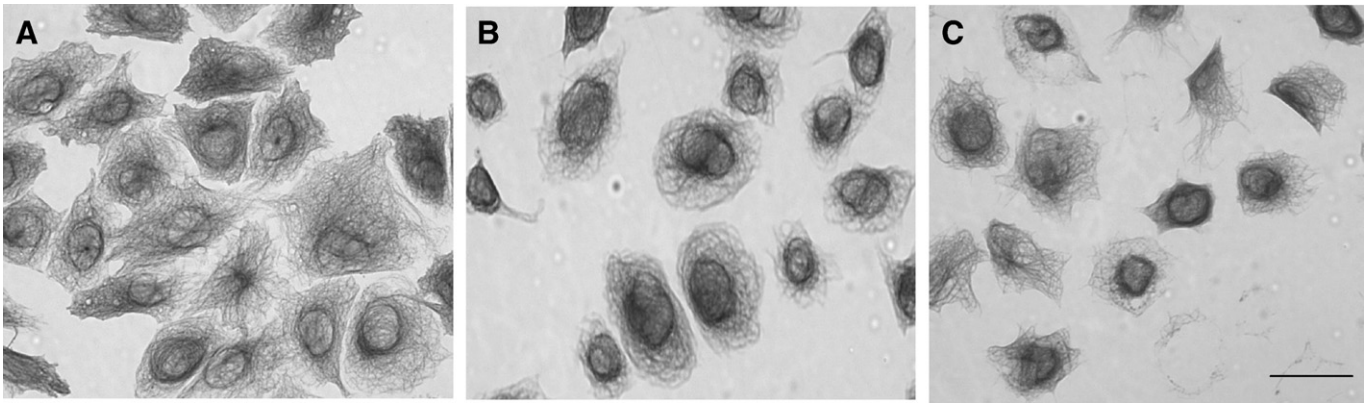

Fig. 9. Effect of zinc sulphate on the microtubule network in 102C5 cells. Immunolabelling with an anti-α tubulin antibody. Cells were untreated (A), or treated for 4 h with 250 μM (B) or 500 μM (C) zinc sulphate. The microtubule network is still present in zinc-treated cells. Scale bar: 25 μm.

deprived conditions. Different culture conditions and the use of a different cell type might explain these differences with the results reported in this study. The present observations investigating the effect of increasing zinc concentrations on tau phosphorylation, tau conformation, and association to microtubules should be extended in further studies on neuronal cells. The cell lines used in this study are however an adequate cellular model to evaluate at first the effect of zinc on tau phosphorylation and its association to microtubules, since these clonal cell lines express tau at a moderate level (by comparison with transiently transfected cells) and tau in these cells is physiologically associated to microtubules. In addition, due to the flat aspect of these cells, the microtubule network is quite spread, allowing an easier estimation of modifications of this network in experimental conditions.

Thus our results suggest that high concentration of zinc might induce increased tau phosphorylation and conformational modifications of tau, typical of early changes in neurons developing neurofibrillary tangles. Interestingly, zinc is highly concentrated in brain areas or in projections to these brain areas that are more selectively affected by the neurofibrillary pathology. The highest chelatable zinc is essentially restricted to the synaptic vesicles of a sub-population of glutamatergic neurons of the dentate gyrus generating mossy fibre boutons in the hippocampus (which store the highest levels of vesicular zinc), and neurons in amygdala nuclei, enthorhinal and pyriform cortices and in associative neocortex. Efferent zinc containing fibres from these regions are in turn directed almost exclusively to cerebral cortex and limbic targets [40]. The hippocampal formation, the perirhinal cortex and the subiculum are the major points of convergence of zinc-containing neurons and thus heavily innervated by zinc-containing buttons and strikingly those regions are severely affected in AD. On the contrary, zinc-containing neurons are generally not found in the spinal cord and in the cerebellum and the latter areas are devoid of neurofibrillary lesions in AD. At the synaptic level zinc is released during glutamatergic neurotransmission and participate to control of post-synaptic proteins like the NMDA and GABA receptors [41]. Ionic zinc is restricted and concentrated into the glutamatergic synaptic vesicle by the ZnT3 transporters residing on the synaptic vesicle membranes of zinc-containing neurons [42]. Accordingly, ZnT3 mRNA expression was observed to be high in the same regions as those where ionic zinc is found. Zinc is strongly suspected to play a role in the development or the enhancement of amyloid deposits. In AD, zinc ions are enriched in the neocortical areas, and even further concentrated into amyloid deposits [3] suggesting that interactions between Aβ and zinc play a role in AD pathogenesis [2,5,14]. Zinc is also found in high concentration in the plaques in the brains of transgenic APP mouse models of AD [30]. We suggest that the abnormally high zinc concentration in amyloid plaques could also play a role in the tau pathology observed in AD. Amyloid plaques are surrounded by abnormal dystrophic neurites and high concentrations of zinc in these neurites as observed by Timm's staining method for zinc [43], could explain the repeated observations of increased tau phosphorylation in dystrophic neurites associated to amyloid deposits in plaques, both in AD [44] and in transgenic APP mice models [45].

In conclusion, this study shows that tau phosphorylation and conformation is modulated by zinc and we suggest that the abnormal extracellular zinc concentration present in Aβ amyloid plaques could play a role in neuronal tau pathology in AD and could explain the preferential development of tau pathology in brain areas rich in zinc in this disease.

Acknowledgments

This study was supported in part by the Interuniversity Attraction Poles program (P6/43) of the Belgian Federal Science Policy Office (BELSPO), the Fonds pour la Recherche Scientifique Médicale (FRSM grants no. 3.4503.06 and 3.4.545.05), the Fondation pour la Recherche sur la Maladie d'Alzheimer/Stichting voor Alzheimer Onderzoek (FRMA/SAO) and the Ligue Alzheimer Association. V.D. was supported by a First Europe grant from the Région Wallonne and the European Commission (n°EP1A320504R0372/215058). We are grateful to Drs S. Kaech and A. Matus (Friedrich Miescher Institute, Basel, Switzerland) for providing us with the tau-EGFP plasmid.

References

[1] D. Religa, D. Strozyk, R.A. Cherny, I. Volitakis, V. Haroutunian, B. Winblad, J. Naslund, A.I. Bush, Elevated cortical zinc in Alzheimer disease, Neurology 67 (2006) 69–75.
[2] C.J. Maynard, A.I. Bush, C.L. Masters, R. Cappai, Q.X. Li, Metals and amyloid-beta in Alzheimer's disease, Int. J. Exp. Pathol. 86 (2005) 147–159.
[3] M.P. Cuajungco, C.J. Frederickson, A.I. Bush, Amyloid-beta metal interaction and metal chelation, Subcell. Biochem. 38 (2005) 235–254.
[4] D.G. Smith, R. Cappai, K.J. Barnham, The redox chemistry of the Alzheimer's disease amyloid beta peptide, Biochim. Biophys. Acta 1768 (2007) 1976–1990.
[5] A.I. Bush, The metallobiology of Alzheimer's disease, Trends Neurosci. 26 (2003) 207–214.
[6] E. Aizenman, A.K. Stout, K.A. Hartnett, K.E. Dineley, B. McLaughlin, I.J. Reynolds, Induction of neuronal apoptosis by thiol oxidation: putative role of intracellular zinc release, J. Neurochem. 75 (2000) 1878–1888.
[7] M.A. Lovell, J.D. Robertson, W.J. Teesdale, J.L. Campbell, W.R. Markesbery, Copper, iron and zinc in Alzheimer's disease senile plaques, J. Neurol. Sci. 158 (1998) 47–52.
[8] A. Boom, R. Pochet, M. Authelet, L. Pradier, P. Borghgraef, F. Van Leuven, C.W. Heizmann, J.P. Brion, Astrocytic calcium/zinc binding protein S100A6 over expression in Alzheimer's disease and in PS1/APP transgenic mice models, Biochim. Biophys. Acta 1742 (2004) 161–168.
[9] C.W. Heizmann, J.A. Cox, New perspectives on S100 proteins: a multi-functional Ca (2+)-, Zn(2+)- and Cu(2+)-binding protein family, Biometals 11 (1998) 383–397.
[10] C.J. Frederickson, S.W. Suh, D. Silva, C.J. Frederickson, R.B. Thompson, Importance of zinc in the central nervous system: the zinc-containing neuron, J. Nutr. 130 (2000) 1471S–1483S.
[11] J. Fukuda, K. Kawa, Permeation of manganese, cadmium, zinc, and beryllium through calcium channels of an insect muscle membrane, Science 196 (1977) 309–311.
[12] X. Huang, M.P. Cuajungco, C.S. Atwood, R.D. Moir, R.E. Tanzi, A.I. Bush, Alzheimer's disease, beta-amyloid protein and zinc, J. Nutr. 130 (2000) 1488S–1492S.
[13] S.B. Roberts, J.A. Ripellino, K.M. Ingalls, N.K. Robakis, K.M. Felsenstein, Non-amyloidogenic cleavage of the beta-amyloid precursor protein by an integral membrane metalloendopeptidase, J. Biol. Chem. 269 (1994) 3111–3116.
[14] A.R. White, K.J. Barnham, A.I. Bush, C.J. Maynard, A.I. Bush, C.L. Masters, R. Cappai, Q.X. Li, C.J. Frederickson, J.Y. Koh, A.I. Bush, Metal homeostasis in Alzheimer's disease. Metals and amyloid-beta in Alzheimer's disease. The neurobiology of zinc in health and disease, Expert. Rev. Neurother. 6 (2006) 711–722.
[15] J.J. Pei, W.L. An, X.W. Zhou, T. Nishimura, J. Norberg, E. Benedikz, J. Gotz, B. Winblad, P70 S6 kinase mediates tau phosphorylation and synthesis, FEBS Lett. 580 (2006) 107–114.
[16] S.W. Suh, K.B. Jensen, M.S. Jensen, D.S. Silva, P.J. Kesslak, G. Danscher, C.J. Frederickson, Histochemically-reactive zinc in amyloid plaques, angiopathy, and degenerating neurons of Alzheimer's diseased brains, Brain Res. 852 (2000) 274–278.
[17] B.W. Doble, J.R. Woodgett, GSK-3: tricks of the trade for a multi-tasking kinase, J. Cell Sci. 116 (2003) 1175–1186.
[18] N. Embi, D.B. Rylatt, P. Cohen, Glycogen synthase kinase-3 from rabbit skeletal muscle. Separation from cyclic-AMP-dependent protein kinase and phosphorylase kinase, Eur. J. Biochem. 107 (1980) 519–527.
[19] S. Lovestone, C.H. Reynolds, D. Latimer, D.R. Davis, B.H. Anderton, J.M. Gallo, D. Hanger, S. Mulot, B. Marquardt, S. Stabel, et al., Alzheimer's disease-like phosphorylation of the microtubule-associated protein tau by glycogen synthase kinase-3 in transfected mammalian cells, Curr. Biol. 4 (1994) 1077–1086.
[20] K. Leroy, A. Boutajangout, J. Richardson, J.N. Octave, S. Lovestone, B.H. Anderton, J.P. Brion, Mutant presenilin 1 proteins induce cell death and reduce tau-dependent processes outgrowth, Neurosci. Lett. 353 (2003) 226–230.
[21] S. Kaech, B. Ludin, A. Matus, Cytoskeletal plasticity in cells expressing neuronal microtubule-associated proteins, Neuron 17 (1996) 1189–1199.
[22] S. Lovestone, D.R. Davis, M.T. Webster, S. Kaech, J.P. Brion, A. Matus, B.H. Anderton, Lithium reduces tau phosphorylation: effects in living cells and in neurons at therapeutic concentrations, Biol. Psychiatry 45 (1999) 995–1003.
[23] J.P. Brion, D.P. Hanger, M.T. Bruce, A.M. Couck, J. Flament-Durand, B.H. Anderton, Tau in Alzheimer neurofibrillary tangles. N- and C-terminal regions are differentially associated with paired helical filaments and the location of a putative abnormal phosphorylation site, Biochem. J. 273 (1991) 127–133.
[24] L. Otvos Jr., L. Feiner, E. Lang, G.I. Szendrei, M. Goedert, V.M. Lee, Monoclonal antibody PHF-1 recognizes tau protein phosphorylated at serine residues 396 and 404, J. Neurosci. Res. 39 (1994) 669–673.
[25] C.L. Weaver, M. Espinoza, Y. Kress, P. Davies, Conformational change as one of the earliest alterations of tau in Alzheimer's disease, Neurobiol. Aging 21 (2000) 719–727.
[26] V. Daubie, C. Nicaise, R. Pochet, Ostesarcoma cell calcium signaling through tissue factor–factor VIIa complex and factor Xa, FEBS Lett. 581 (2007) 2611–2615.

[27] I. Grundke-Iqbal, K. Iqbal, Y.C. Tung, M. Quinlan, H.M. Wisniewski, L.I. Binder, Abnormal phosphorylation of the microtubule-associated protein tau (tau) in Alzheimer cytoskeletal pathology, Proc. Natl. Acad. Sci. U. S. A. 83 (1986) 4913–4917.
[28] J. Biernat, E.M. Mandelkow, C. Schroter, B. Lichtenberg-Kraag, B. Steiner, B. Berling, H. Meyer, M. Mercken, A. Vandermeeren, M. Goedert, et al., The switch of tau protein to an Alzheimer-like state includes the phosphorylation of two serine-proline motifs upstream of the microtubule binding region, EMBO J. 11 (1992) 1593–1597.
[29] A.I. Bush, R.E. Tanzi, The galvanization of beta-amyloid in Alzheimer's disease, Proc. Natl. Acad. Sci. U. S. A. 99 (2002) 7317–7319.
[30] J.Y. Lee, T.B. Cole, R.D. Palmiter, S.W. Suh, J.Y. Koh, Contribution by synaptic zinc to the gender-disparate plaque formation in human Swedish mutant APP transgenic mice, Proc. Natl. Acad. Sci. U. S. A. 99 (2002) 7705–7710.
[31] Y. Jia, J.M. Jeng, S.L. Sensi, J.H. Weiss, Zn2+ currents are mediated by calcium-permeable AMPA/kainate channels in cultured murine hippocampal neurones, J. Physiol. 543 (2002) 35–48.
[32] R. Ilouz, O. Kaidanovich, D. Gurwitz, H. Eldar-Finkelman, Inhibition of glycogen synthase kinase-3beta by bivalent zinc ions: insight into the insulin-mimetic action of zinc, Biochem. Biophys. Res. Commun. 295 (2002) 102–106.
[33] W.L. An, C. Bjorkdahl, R. Liu, R.F. Cowburn, B. Winblad, J.J. Pei, Mechanism of zinc-induced phosphorylation of p70 S6 kinase and glycogen synthase kinase 3beta in SH-SY5Y neuroblastoma cells, J. Neurochem. 92 (2005) 1104–1115.
[34] K. Leroy, A. Boutajangout, M. Authelet, J.R. Woodgett, B.H. Anderton, J.P. Brion, The active form of glycogen synthase kinase-3beta is associated with granulovacuolar degeneration in neurons in Alzheimer's disease, Acta Neuropathol. (Berl.) 103 (2002) 91–99.
[35] K. Leroy, Z. Yilmaz, J.P. Brion, Increased level of active GSK-3beta in Alzheimer's disease and accumulation in argyrophilic grains and in neurones at different stages of neurofibrillary degeneration, Neuropathol. Appl. Neurobiol. 33 (2007) 43–55.
[36] R.M. Brady, R.P. Zinkowski, L.I. Binder, Presence of tau in isolated nuclei from human brain, Neurobiol. Aging 16 (1995) 479–486.
[37] M.M. Black, T. Slaughter, S. Moshiach, M. Obrocka, I. Fischer, Tau is enriched on dynamic microtubules in the distal region of growing axons, J. Neurosci. 16 (1996) 3601–3619.
[38] S. Lovestone, C.L. Hartley, J. Pearce, B.H. Anderton, Phosphorylation of tau by glycogen synthase kinase-3 beta in intact mammalian cells: the effects on the organization and stability of microtubules, Neuroscience 73 (1996) 1145–1157.
[39] K. Leroy, R. Menu, J.L. Conreur, R. Dayanandan, S. Lovestone, B.H. Anderton, J.P. Brion, The function of the microtubule-associated protein tau is variably modulated by graded changes in glycogen synthase kinase-3beta activity, FEBS Lett. 465 (2000) 34–38.
[40] M.K. Christensen, C.J. Frederickson, Zinc-containing afferent projections to the rat corticomedial amygdaloid complex: a retrograde tracing study, J. Comp. Neurol. 400 (1998) 375–390.
[41] C.J. Frederickson, D.W. Moncrieff, Zinc-containing neurons, Biol. Signals 3 (1994) 127–139.
[42] D.H. Linkous, J.M. Flinn, J.Y. Koh, A. Lanzirotti, P.M. Bertsch, B.F. Jones, L.J. Giblin, C.J. Frederickson, Evidence that the ZNT3 protein controls the total amount of elemental zinc in synaptic vesicles, J. Histochem. Cytochem. 56 (2008) 3–6.
[43] M. Stoltenberg, M. Bruhn, C. Sondergaard, P. Doering, M.J. West, A. Larsen, J.C. Troncoso, G. Danscher, Immersion autometallographic tracing of zinc ions in Alzheimer beta-amyloid plaques, Histochem. Cell Biol. 123 (2005) 605–611.
[44] M.A. Kurt, D.C. Davies, M. Kidd, K. Duff, D.R. Howlett, Hyperphosphorylated tau and paired helical filament-like structures in the brains of mice carrying mutant amyloid precursor protein and mutant presenilin-1 transgenes, Neurobiol. Dis. 14 (2003) 89–97.
[45] A. Boutajangout, M. Authelet, V. Blanchard, N. Touchet, G. Tremp, L. Pradier, J.P. Brion, Characterisation of cytoskeletal abnormalities in mice transgenic for wild-type human tau and familial Alzheimer's disease mutants of APP and presenilin-1, Neurobiol. Dis. 15 (2004) 47–60.